The segregation of recycled basaltic material within mantle plumes explains the detection of the X-Discontinuity beneath hotspots

2D geodynamic simulations

Martina Monaco*[1], Juliane Dannberg[1], René Gassmöller[1]

DI25B-0028

[1], University of Florida, Dept. of Geological Sciences; *martinamonaco@ufl.edu

OUTLINE

Increasing evidence points towards a thermochemical mantle plume beneath the Hawaiian hotspot. The detection of the X-Discontinuity at depths between 250 and 350 km is of particular interest for constraining its composition. The origin of the X-Discontinuity is often attributed to two phase transitions: (1) the transition from orthoenstatite to high-pressure clinoenstatite in (Mg,Fe)SiO_3 pyroxene, and (2) the coesite to stishovite phase transition in SiO_2. The availability of silica at these depths could be explained if mantle plumes carry eclogite, which would affect their dynamics.

Previous studies postulated that plumes may carry no more than 15% eclogite. We adopt a new approach, and set up a a model featuring two compositions: a background *pyrolite* with *basaltic chemical heterogeneities* flowing in. We explore the feasibility of the accumulation of such basaltic material within a mantle plume, and employ a wide array of densities and viscosities to analyze the possible dynamics behind basalt accumulations greater than 15%. We find that:

1. Plumes can accumulate substantially more than 15% eclogite for extended amounts of model times
2. The phase transition between coesite and stishovite can explain the occurrence of the X-Discontinuity
3. The sustained accumulation of basaltic heterogeneities in the depth range between 300 and 410 km can reconcile the strong reflections observed in seismological studies and shed a light on the plume dynamics.

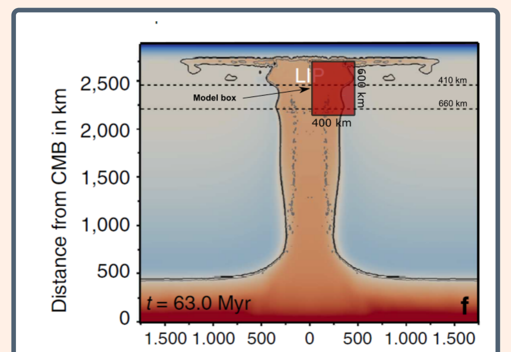

Figure 1: Thermochemical plume sketch — Model box highlighted. From [1].

Our innovative two-composition approach, coupled with the observation of seismic discontinuities beneath Hawaii, offers a unique opportunity to analyze the dynamics of basalt accumulation in mantle plumes.

1. BASIC EQUATIONS & MODEL GEOMETRY

The convection in the Earth's mantle is governed by the conservation of *mass* (Equation 1) and *momentum* (Equation 2). We use the geodynamic modeling software ASPECT to solve the incompressible Stokes system for pressure and velocity ([2], [3], [4].

Our model includes chemical heterogeneities in the form of spherical basaltic inclusions within a pyrolitic matrix. We used the PIC (particle-in-cell, [5]) method to model the transport of the basaltic material, which is described by the *advection equation* (Equation 3).

$$\nabla \cdot \mathbf{u} = 0 \qquad (1)$$

$$-\nabla \cdot [2\eta\dot{\varepsilon}'] + \nabla p = \rho \mathbf{g} \qquad (2)$$

$$\frac{\partial C}{\partial t} + \mathbf{u} \cdot \nabla C = 0 \qquad (3)$$

Figure 2: Basic Equations. ρ is the density, $\mathbf{u}$ the velocity vector, η the viscosity, p the pressure, g the gravity, and $\dot{\varepsilon}'$ the deviatoric strain rate tensor. In the advection equation, C is the composition, specifically the basalt fraction. We compute the fraction of pyrolite as $1 - C$, so that we do not need to solve a separate equation for it.

The model setup consists of a 2D box, 400 km in width and 600 km in depth, representing a section of the plume conduit (Figure 1). The top of the box is located at 110 km depth, as we do not take into account the lithosphere. Based on the different density profiles shown in Figure 3, we define three model series: the (1) *100 series*, the (2) *Aoki series*, and the (3) *Hefesto series*.

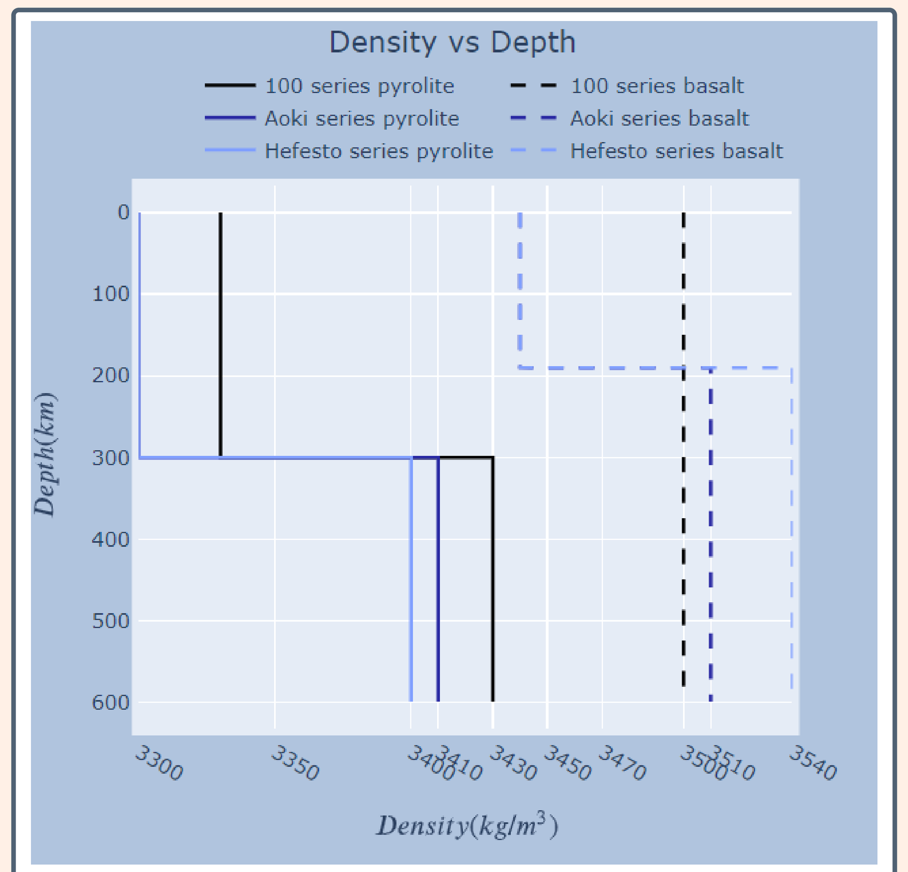

Figure 3: Starting arrays of density vs depth for the three series. The depth range is computed with respect to the box reference. To translate it into real depth, one must add 110 km to each value.

2. INITIAL & BOUNDARY CONDITIONS

All three series include a phase transition that cuts the box in two equal halves. This represents the *olivine-wadsleyite* phase transition that occurs in the mantle at 410 km depth.

1. The 100 series is our simplest case, and only features a single value of basalt density throughout the model box. We use this series as a baseline to predict and analyze the behavior of the heterogeneities in the absence of a phase transition in the basalt.
2. The Aoki series adopts density values from [6]
3. The Hefesto series adopts density values from [7] In addition to the 410 km depth phase transition, they feature the coesite-stishovite phase transition in the basaltic material, such that the basalt has two different density values above and below it. We placed the transition at 190 km depth in the model box (300 km depth in the real mantle). In both series, the basalt above the coesite-stishovite transition assumes a density of 3440 kg/m^3.

Our model is a section of a plume conduit. The material moves upwards, faster in the hot center (left hand side) compared to the colder margin. We prescribe the following boundary conditions.

1. Top and left sides: boundary velocity of 10 cm/yr vertically, 0 horizontally.
2. Right side: unrestrained velocity tangential to the boundary, 0 velocity normal to the boundary (free slip).
3. Bottom boundary: open and stress-free, material can flow in according to the forces acting in the model. Fixed composition.

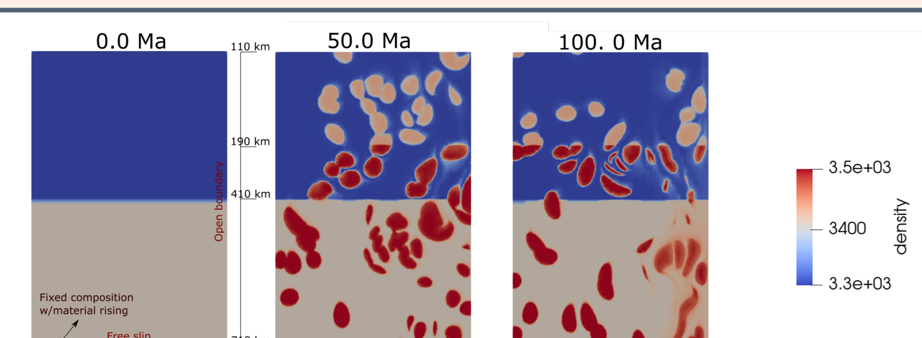

Figure 4: Model setup. Background colors indicate the density. The depth range is scaled to real depth, such that the top of the model box corresponds to 110 km depth in the mantle. We neglect the role of the lithosphere and the 660 km depth phase transition.

3. RESULTS: INFLUENCE OF THE PYROLITE VISCOSITY

Our analysis focuses on the fraction of basalt present between 300 and 410 km depth. This is motivated by the very reason of our investigation: can a plume accumulate enough basalt in the depth ranges that correspond to the X-discontinuity? In order for the discontinuity to be seismically discerned, basalt percentages as high as 40% are required.

The behavior of the models is first and foremost determined by the *background viscosity*. Depending on the pyrolite viscosity, we identify three different regimes: (1) *fully sinking*, (2) *fully rising*, and (3) *mixed*, which features rising, sinking, and ponding together.

1. The *fully sinking* regime occurs for the lowest pyrolite viscosity values. The gravity forces acting on the dense heterogeneities exceed the frictional forces that would allow them to be carried upwards with the plume (per the Stokes law). The heterogeneities sink shortly after entering the box, undergoing significant deformation, and few stretched remnants make it above the 410 discontinuity, thus eventually escaping the box. These are the models with the lowest basalt percentages.
2. On the opposite side of the spectrum, we identify the *fully rising regime*. The pyrolite viscosity is so high that all chemical heterogeneities rise with the same velocity as the background, without substantial deformation. The fraction of basaltic material in the model box remains close to the fraction of basalt prescribed by the boundary conditions.
3. The models in the *mixed* regime feature intermediate pyrolite viscosities. In this case, the basaltic heterogeneities rise, sink, and pond cyclically around the phase transitions, especially in the depth range between 300 and 410 km, corresponding to the coesite—stishovite and olivine—wadsleyite phase transitions. This behavior can be explained by the density contrast between basalt and pyrolite. The associated downwards gravitational force is largest between these transitions. Because the friction force stays the same, the heterogeneities can be carried upwards more easily below 410 km and above 300 km depth, but are more likely to sink in between. This makes their ascent path irregular, as they get entrained by the background flow to a variable degree. Depending on their position with respect to the open boundary, the phase transition, and the degree of clustering of individual inclusions, they either sink, rise or pond. As basalt cyclically accumulates around 300 and 410 km depth, at times the fraction of basalt at this depth substantially exceeds the average fraction of basalt flowing in at the bottom of the model.

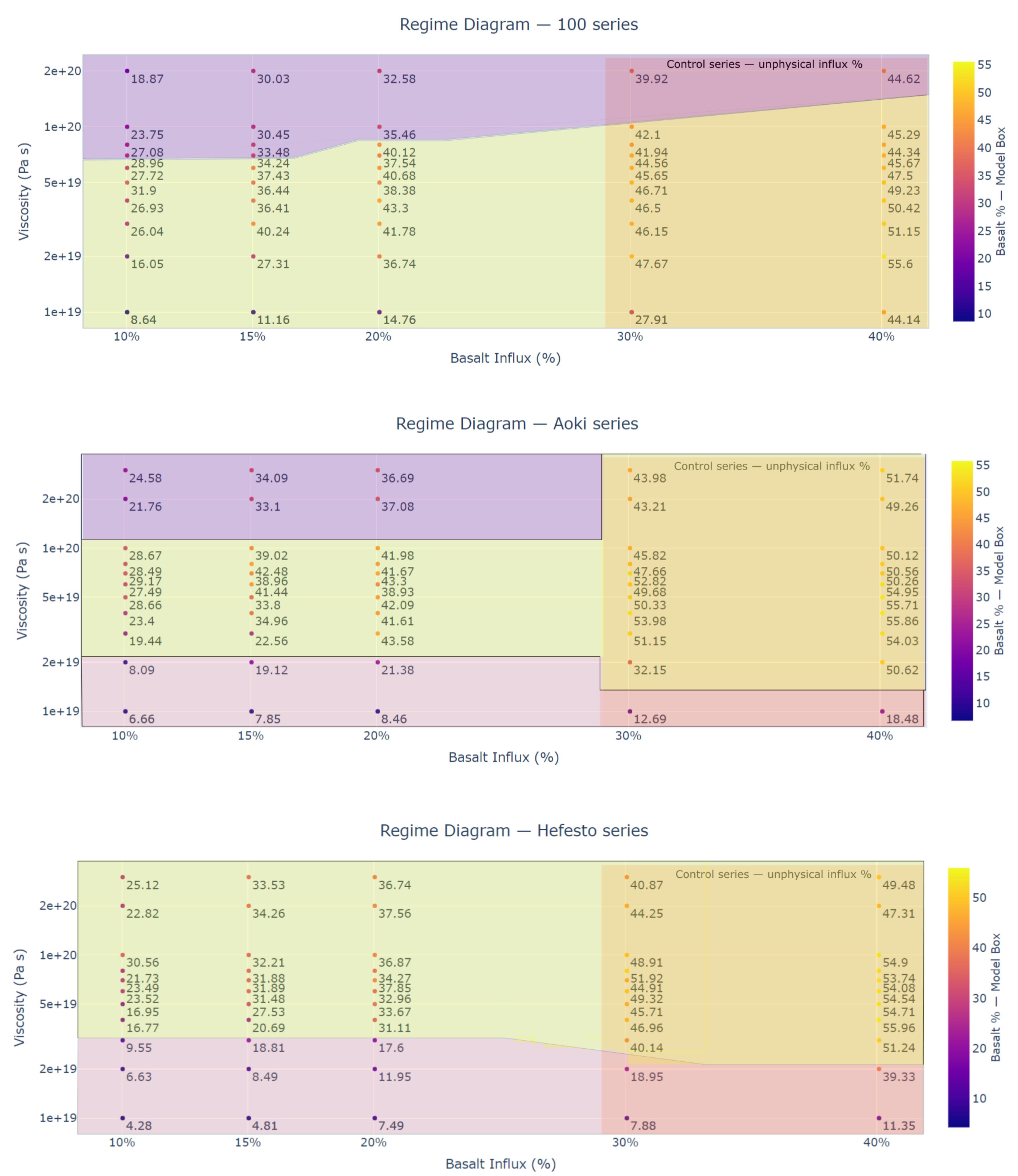

Figure 5: Regime diagrams for the three different model series. Shade colors outline the three regimes: pink for fully sinking, yellow for mixed, and purple for fully rising. The label on each dot represents the highest basalt percentage in the depth range of the phase transition(s) attained in that model run. The 100 series does not feature a fully sinking regime for the viscosity values displayed.

4. INFLUENCE OF THE DENSITY AND EVOLUTION OVER TIME

The second determining factor in the model evolution are the density profiles of pyrolite and basalt.

1. The 100 series does not feature the coesite-stishovite transition and has the lightest basalt (3500 kg/m^3). The patterns of rising and sinking are very straightforward, as the percentages of basalt over time show a consistent increase after enough heterogeneities enter the box, with only minor periodical declines due to the statistical distribution of the basalt. The models featuring viscosity values below 7×10^{19} are in the mixed regime, and show accumulations as high as 40% and no lower than 26% of basalt in the layer around and above the 410 km phase transition.
2. The Aoki and Hefesto series show very different patterns of basalt accumulation. This is a direct consequence of the lower densities of the pyrolite compared to an overall higher density basaltic material. As a result, all transitions between the regimes are shifted towards higher background viscosities. Moreover, the presence of two phase transitions, and the employment of two different density values for the basalt above and below them creates larger density contrasts. As a result, in the mixed regime the chemical heterogeneities slow down and pond around the 410 phase transition. The Hefesto series shows a shift upwards in the onset of the mixed regime, which starts at 4×10^{19} Pa s pyrolite viscosity. Secondly, the basalt percentages in the Hefesto series are up to 20% lower than in similar runs for the Aoki series (e.g. for pyrolite viscosities of 4×10^{19} Pa s), and never attain values higher than 37.56% for any of the physical combinations of initial parameters employed in this study.

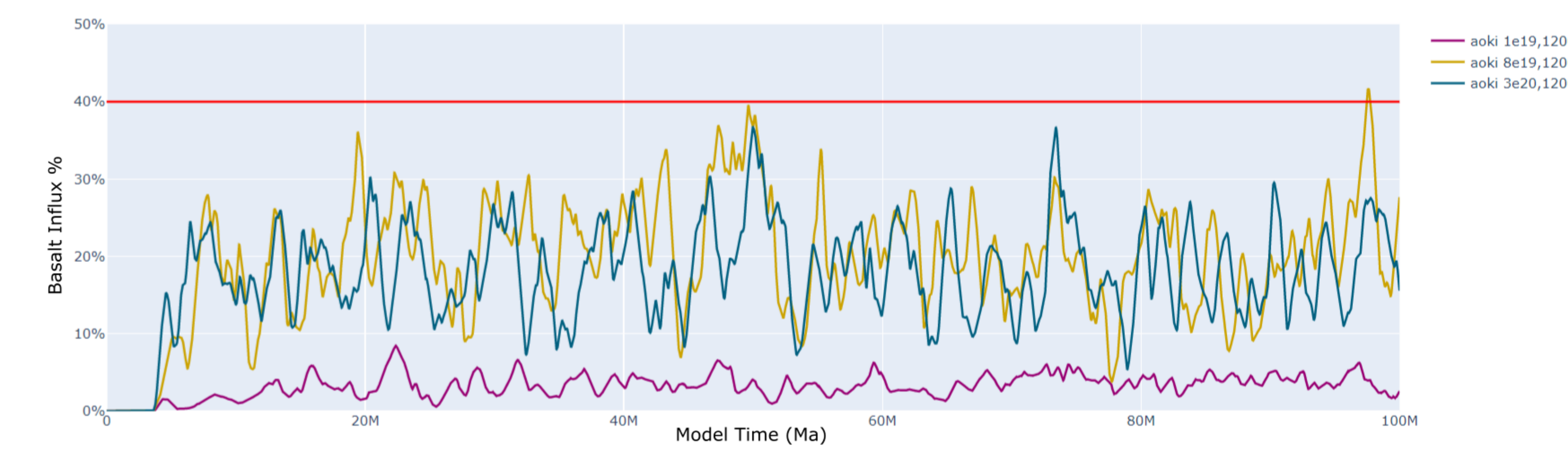

Figure 6: Evolution over time of three selected model runs from the Aoki series.

5. DISCUSSION

1. Our results show that there is a parameter regime that sustains basalt percentages above 30% and up to slightly above 40% in the layer between the X-Discontinuity and the 410 discontinuity.
2. For viscosity values compatible with those of the Hawaiian plume, great density contrasts exist in the depth range between 300 and 410 km depth. These provide a viable mechanism for the cyclical ponding of higher-density material.
3. We observe high percentages of basalt in the model box in both the *mixed* and the *fully rising* regimes, although the underlying mechanisms are very different. In the mixed regime, the basalt ponds in the depth range between the two discontinuities for a few million years. On the other hand, when the basalt fully rises without undergoing significant deformation, the amount of basaltic material is similar throughout the whole depth range at all times, but never substantially exceeds the fraction of basalt flowing in from the bottom.
4. Although the *fully rising* regime may be relevant for some plumes, we believe that some ponding is required in order to match the seismological observations of the X-discontinuity.

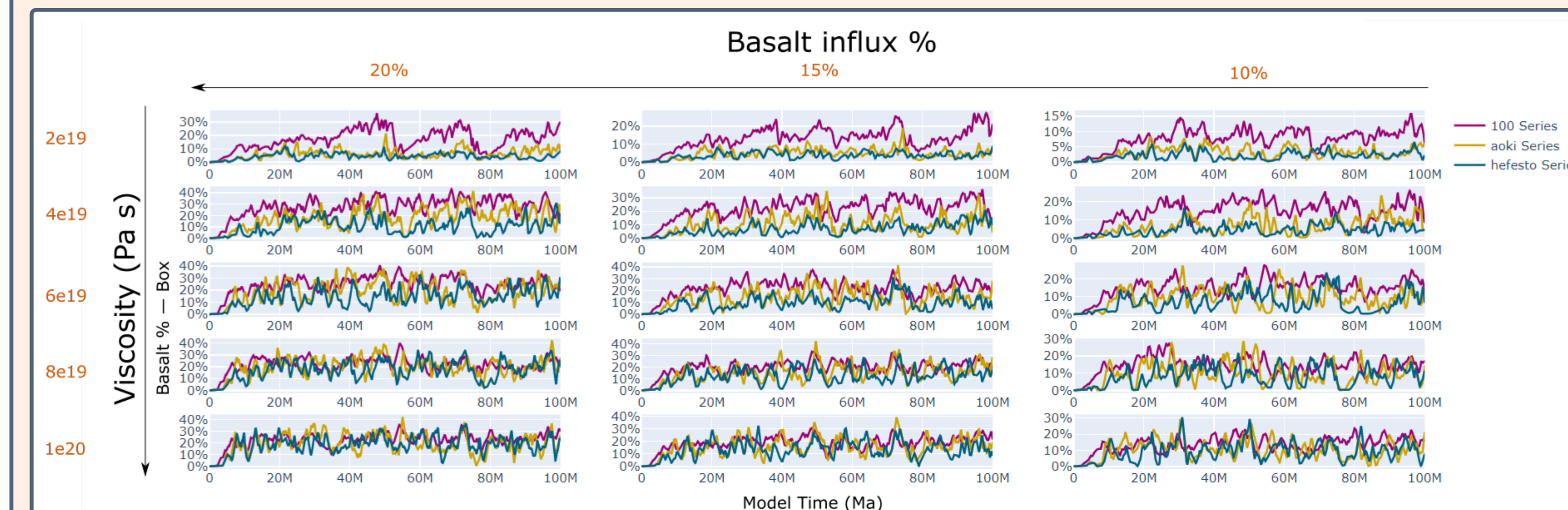

Figure 7: Model evolution for all series. The viscosity (y axis) is plotted versus the model time (x axis) for the three relevant percentages of basalt influx.

CONCLUSIONS

In this study, we simulate the ascent of dense chemical heterogeneities within a plume conduit to test the feasibility of ponding and accumulation of basaltic material within a mantle plume. We have developed geodynamic models adopting a radically new approach, assuming that mixing of the higher density chemical heterogeneities that are entrained in the plume occurs on a length scale that is large enough to allow them to move relative to the background material. Our main findings are:

- Plumes can accumulate up to 40% eclogite at depths compatible with the appearance of the X-Discontinuity
- Such accumulations happen within the *mixed regime*
- The ponding of higher density material can explain the seismological observations of the X-Discontinuity beneath the Hawiian hotspot
- Our models do not predict peaks of basaltic accumulation above 55% (for any of the density and viscosity values). They however show the feasibility of a 40% basalt accumulation, though for not sustained periods of model time
- Additional studies will be performed to explore the mechanisms of basalt ponding under mantle-like conditions

REFERENCES

We thank the Computational Infrastructure for Geodynamics (geodynamics.org) which is funded by the National Science Foundation under award EAR-0949446 and EAR-1550901 for supporting the development of ASPECT. This work was also supported by the NSF grant EAR-1925677.

References

[1] Dannberg, J. & Sobolev, S. V. Low-buoyancy thermochemical plumes resolve controversy of classical mantle plume concept. *Nature Communications* **6** (2015).

[2] Kronbichler, M., Heister, T. & Bangerth, W. High accuracy mantle convection simulation through modern numerical methods. *Geophysical Journal International* **191**, 12–29 (2012).

[3] Heister, T., Dannberg, J., Gassmöller, R. & Bangerth, W. High accuracy mantle convection simulation through modern numerical methods–ii: realistic models and problems. *Geophysical Journal International* **210**, 833–851 (2017).

[4] Bangerth, W. *et al.* Aspect v2.3.0 (2021). URL https://doi.org/10.5281/zenodo.5131909.

[5] Gassmöller, R., Lokavarapu, H., Heien, E., Puckett, E. G. & Bangerth, W. Flexible and scalable particle-in-cell methods with adaptive mesh refinement for geodynamic computations. *Geochemistry, Geophysics, Geosystems* **19**, 3596–3604 (2018). URL https://doi.org/10.1029/2018GC007508.

[6] Aoki, I. & Takahashi, E. Density of morb eclogite in the upper mantle. *Physics of the Earth and Planetary Interiors* **143-144**, 129–143 (2004).

[7] Stixrude, L. & Lithgow-Bertelloni, C. Thermodynamics of mantle minerals - ii. phase equilibria. *Geophysical Journal International* **184**, 1180–1213 (2011).